analytical chemistry

pubs.acs.org/ac Article

Mitochondria-Immobilized Unimolecular Fluorescent Probe for Multiplexing Imaging of Living Cancer Cells

Nansong Zhu, Xiaolei Guo, Shirui Pang, Yulei Chang,* Xiaomin Liu, Zhan Shi,* and Shouhua Feng

Cite This: *Anal. Chem.* 2020, 92, 11103−11110 Read Online

ACCESS | Metrics & More | Article Recommendations | Supporting Information

ABSTRACT: Cancer incidence and mortality are fast growing worldwide. Recently, multiplexing imaging methods have been reported to be vital for cancer diagnosis and therapy. Fluorescence imaging, which has intrinsic capabilities for multiplexing imaging, is suitable and ripe for cancer imaging. In biomedical research, using a single probe for multiplexing imaging can avoid larger invasive effects and ensure the same spatiotemporal distributions and metabolisms of the probes, which has advantages over using multiple probes. Therefore, developing unimolecular fluorescent probes for multiplexing imaging of living cancer cells is meaningful. We herein report a unimolecular fluorescent probe (ZED) that simultaneously detects cysteine/homocysteine, hypochlorous acid, mitochondrial membrane potential ($\Delta\psi_m$), and opening of the mitochondrial permeability transition (MPT) pore in cells. These four analytes are key indicators predominantly associated with multiple aspects of carcinogenesis and cancer therapy in living cells. Besides, ZED also differentiates MCF-7 cells from HBL-100 cells. The sensing process is fast, selective, and sensitive in living cancer cells. As far as we know, ZED is the first probe that simultaneously detects four analytes in cells and the first probe that simultaneously detects $\Delta\psi_m$ and opening of the MPT pore in mitochondria.

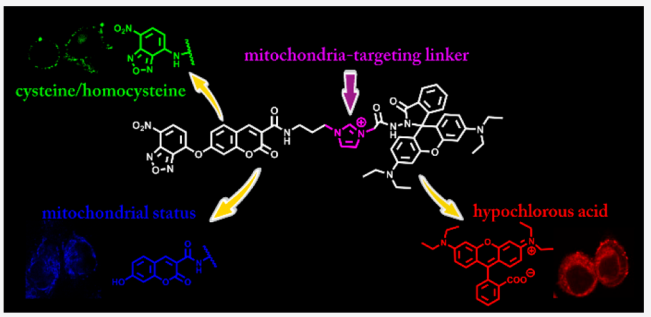

Cancer is the first or second leading cause of death in many countries according to estimates from the World Health Organization (WHO) in 2015, and tens of millions of people die of different cancers every year.[1] As an evolving technology, optical imaging has been frequently used in biomedical research for decades and suitable for cancer imaging due to its high temporal and spatial resolutions.[2] Fluorescence imaging using "contrast agents", which provides real-time analysis in cells, is one of the most popular and powerful optical imaging modalities.[3] To date, fluorescence imaging is also the most powerful and indispensable intraoperative guidance for cancer surgery.[4,5]

Recently, multiplexing imaging methods have been proposed to be important for cancer diagnosis and therapy.[6] Multiplexing imaging is a new term in cancer imaging. It allows scientists to simultaneously obtain multifunctional information in the imaged systems, which improves the accuracy of cancer diagnosis and enables real-time tracking on the therapeutic efficacy.[7] In addition to the advantages in cancer imaging, fluorescence imaging also has intrinsic capabilities for multiplexing imaging.[8] As known to all, fluorophores produce signals with two parameters, the wavelength and signal intensity. This unique characteristic allows multiple fluorescent contrast agents, which have different excitation and emission wavelengths, to be resolved simultaneously. Since accurate cancer diagnosis and therapy remain challenging in biomedical research, it is meaningful to develop fluorescent probes for multiplexing imaging of cancer cells.

Mitochondrion is an organelle well-studied over the past decades. Mitochondrial membrane potential ($\Delta\psi_m$) guarantees normal mitochondrial function, and mitochondrial dysfunction can cause many diseases.[9] In human malignant cells, the $\Delta\psi_m$ is higher than that in normal cells, which is a well-known characteristic of cancer cells.[10] Recently, mitochondrion is recommended as the vital target of reactive oxygen species (ROS), while mitochondrial dysfunction caused by ROS is developed as a rational cancer therapy.[11−13] For example, hypochlorous acid (HOCl), one of the ROS,[14] can selectively induce apoptosis in cancer cells, which is an important apoptosis-inducing pathway for cancer therapy.[15,16] Meanwhile, HOCl is also implicated in the DNA-damaged process that contributes to the carcinogenesis.[17] In addition, the levels of cysteine (Cys) and homocysteine (Hcy) are also associated with multiple aspects of carcinogenesis and cancer therapy in cells.[18−23] Within this context, there is no doubt that the

Received: March 9, 2020
Accepted: July 14, 2020
Published: July 14, 2020

https://dx.doi.org/10.1021/acs.analchem.0c01046
Anal. Chem. 2020, 92, 11103−11110

Scheme 1. Structure of ZED and Its Stimulus-Response Performances

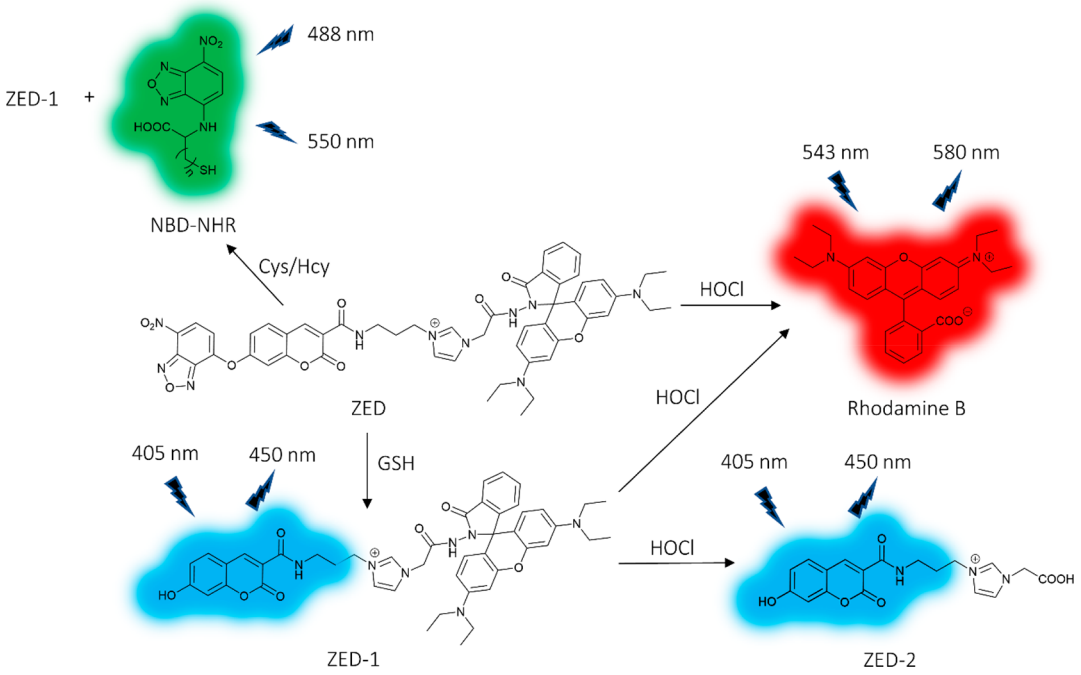

design and development of fluorescent probes, which can simultaneously sense Cys/Hcy, HOCl and mitochondrial status in cells, is meaningful for cancer diagnosis and therapy. To date, many fluorescent probes aimed at Cys/Hcy, HOCl and mitochondrial status have been reported.[24−36] However, none of them can simultaneously sense these analytes in cells. Futhermore, in terms of mitochondrial status, only one fluorescence imaging method for detecting opening of the mitochondrial permeability transition (MPT) pore has been reported.[37] This quenching method involving a fluorescent dye (calcein AM) and a quenching agent (Co^{2+}) is complex to be operated. Hence, exploiting an easy way involving only one fluorescent contrast agent to sense opening of the MPT pore still remains challenging. Besides, no fluorescent probe that can simultaneously detect $\Delta\psi_m$ and opening of the MPT pore has been reported so far. Considering the important roles of $\Delta\psi_m$ and opening of the MPT pore in cancer therapy,[38−40] the development of fluorescent probes for the simultaneous detection of $\Delta\psi_m$ and opening of the MPT pore in mitochondria is also meaningful.

We herein report a probe (ZED) to simultaneously detect Cys/Hcy, HOCl, $\Delta\psi_m$, and opening of the MPT pore with little cross-talk in living cells. To the best of our knowledge, ZED is the first probe that simultaneously detects four analytes in cells and the first probe that simultaneously detects $\Delta\psi_m$ and opening of the MPT pore in mitochondria. Structure of ZED and its stimulus-response performances are illustrated in Scheme 1. The construction of the probe is NBD-Coumarin-Imidazolium salt-Rhodamine in short. ZED's derivate without NBD part is called ZED-1, without either NBD or rhodamine part is called ZED-2. The NBD, coumarin and rhodamine are three parts for sensing Cys/Hcy, mitochondrial status and HOCl, respectively. The imidazolium salt is a cationic linker among fluorophores, which assists ZED to target mitochondria as well. It is also a probable mitochondria-immobilized group as imidazole and imidazolium salt can react with disulfide at 2-position,[41,42] and disulfide bonds are formed in the intermembrane space of mitochondria.[43] Using imidazolium salt as a multifunctional linker among fluorophores simplifies molecular structure, shortens synthesis route, reduces molecular weight and improves water solubility, which provides an easy way to synthesize multifunctional probes. Since other probes can be generated from ZED by simply changing one or several of the three sensing parts, the skeletal structure of ZED is also valuable.

In biomedical research, it is important to develop unimolecular probes for multiplexing imaging, because using a single probe may overcome some drawbacks of using multiple probes, such as (1) time-consuming, (2) complex to be operated, (3) potential cross-talk between different probes, (4) larger invasive effects, and (5) different spatiotemporal distributions and metabolisms of the probes.[44] Although these drawbacks may be tackled by encapsulating multiple probes into a microbead, yet a carefully formulated ratio of the probes is needed for accurate sensing, which makes it not easy to synthesize and reproduce the microbeads.[8,45] Besides, it is also challenging to develop unimolecular probes for multiplexing imaging, because the signals should have as little cross-talk as possible and be distinguishable from each other, which is difficult to be fulfilled in a single probe containing multiple fluorophores. Only a few reports about duplex imaging with cross-talk free signals have been reported.[46−50] In addition, the design, synthesis and application of unimolecular probes for multiplexing imaging can also help scientists to understand the interactions between different fluorophores from a single molecule in solutions and biological environments, which can allow scientists to come up with more ideas about constructing these intricate probes and eventually promote the development of new multifunctional probes. In a word, no matter from the perspective of practical applications or that of scientific developments, it is of significance to develop unimolecular probes for multiplexing imaging.

https://dx.doi.org/10.1021/acs.analchem.0c01046
Anal. Chem. 2020, 92, 11103−11110

EXPERIMENTAL SECTION

Materials and Methods. All solvents were reagent grade. Unless otherwise noted, all reagents were purchased from commercial suppliers and used without further purification. Some of the ROS were generated in situ according to the literature.[47] Twice-distilled water was used in all experiments. ^{1}H NMR and ^{13}C NMR spectra were recorded using a Bruker spectrometer (400 and 100 MHz, respectively). UV/vis spectra were recorded on a U-4100 spectrophotometer. The fluorescence spectra were recorded on an Edinburgh spectrofluorimeter equipped with both continuous (450 W) and pulsed xenon lamps. Liquid Chromatogram-High Resolution Mass Spectra (LC-HRMS) were recorded using a Bruker spectrometer. Confocal images were performed on a confocal laser scanning microscope (Nikon, Japan). TLC analysis was conducted on silica gel plates and flash column chromatography was carried out on silica gel (mesh 200−300).

Absorbance and Fluorescence Measurements. The stock solutions of 5 mM ZED or ZED-1 were freshly prepared in dry DMSO and stored at −20 °C before use. The stock solutions were directly diluted with 1000 times water. Unless otherwise noted, all absorbance and fluorescence measurements were carried out at room temperature in 50 mM PBS buffers (pH 7.4 or pH 8.0, 0.1% DMSO). After mixing with analytes and then standing for suitable time at room temperature, the reaction solutions were transferred into a 1 cm quartz cell to measure the absorbance or fluorescence. The time-dependent fluorescence experiments were carried out in situ in a 1 cm quartz cell.

Cell Culture and Confocal Imaging. Cells were cultured in glass-bottom dishes in DMEM supplemented with 10% (v/v) FBS at 37 °C under a humidified atmosphere containing 5% CO_2. All parallel tests were from the same inoculation density and the same growth time. Cells in the logarithmic phase were used throughout all experiments. Cells were treated with 5 μM ZED in PBS buffers (10 mM, pH 7.4, 0.1% DMSO), HOCl in PBS buffers (10 mM, pH 7.4), and other commercial reagents in serum-free DMEM for indicated time before imaging. Confocal images were carried out in situ in glass-bottom culture dishes with PBS buffers (10 mM, pH 7.4) or a colorless DMEM medium and recorded with a confocal laser scanning microscope (Nikon, Japan).

Determination of the Detection Limits. The detection limits were determined from the fluorescence experiments. The detection limits were calculated with the following equation: Detection limit = $3\sigma/k$, where σ is the standard deviation of the blank measurements and k is the slope of the fluorescence intensities over the concentrations of the analytes.

RESULTS AND DISCUSSION

As a starting point, the stimulus-response performances of ZED are expounded briefly according to Scheme 1. After reacting with glutathione (GSH) or Cys/Hcy, ZED turned into ZED-1 (Figure S1) generating a blue fluorescence F_{405} from the released 7-hydroxycoumarin. Different from GSH, Cys/Hcy further generated a green fluorescence F_{488} from NBD-NHR during the reactions. F_{488} had great selectivity to Cys/Hcy over other biological relevant analytes in cuvettes (Figure S2). Although Cys/Hcy and GSH consumes ZED competitively, the green fluorescence can still be partly turned on in the presence of excess amounts of GSH through a reversible S_NAr substitution,[51] showing that NBD is capable of detecting Cys/Hcy in cells. To date, there are many reports about sensing Cys/Hcy in cells using the NBD moiety,[52−56] and the sensing mechanisms have been well discussed in literature.[57,58] Apart for the response toward thiols, ZED and its derivate, ZED-1, also reacted with HOCl generating a red fluorescence F_{543} from Rhodamine B (Figure S3). F_{543} also had great selectivity to HOCl over other biological relevant analytes in cuvettes (Figure S4). Similar reports and the sensing mechanisms have been well discussed in literature too.[59−61]

As the reaction of ZED and GSH went on, F_{405} reached almost the largest fluorescence intensity at 90 s (Figure S5), and the intensity at 270 s was nearly equal to that of 7-hydroxycoumarin in ZED-1 (Figure S6). This quick and complete generation of F_{405} indicated that ZED-1 would be formed rapidly and totally in cells due to the high GSH concentration in cytoplasm.[62] As expected, F_{405} was turned on brightly in MCF-7 cells after incubation with ZED for 10 min (Figure 1a). The fluorescence intensity also remained almost

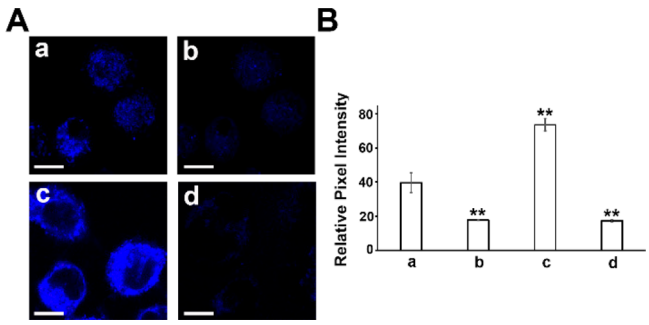

Figure 1. Response of ZED to mitochondrial status in cells. (A) Images of the cells. (a) MCF-7 cells incubated with 5 μM ZED for 10 min. (b) MCF-7 cells incubated with 5 μM ZED for 10 min and then treated with 50 μM CCCP for 20 s. (c) MCF-7 cells incubated with 5 μM ZED for 10 min and then treated with 50 μM CCCP for 2 h. (d) HBL-100 cells incubated with 5 μM ZED for 10 min. Images were recorded using excitation wavelength of 405 nm, and band-path emission filter at 417−477 nm. (B) Relative pixel intensity of the related images in (A). The results are presented as mean ± standard deviation (n = 3). Significant differences (**p < 0.01) are performed by Student's t-test. Scale bar: 10 μm.

unchanged within 15 min (Figure S7), confirming the rapid and total conversion of ZED to ZED-1 in cells. The short incubation time also showed that ZED had good cell permeability. Repeated tests were also carried out to confirm the good cell permeability of ZED (Figure S8). According to the CCK assays, the cell viability did not change much after incubation with ZED (Figure S9), indicating ZED also had good biocompatibility.

In general, cationic dyes are driven into mitochondria by the plasma and mitochondrial membrane potentials,[10] so we first investigated whether F_{405} was localized in mitochondria. F_{405} was quenched in cells when the cells were costained with Mito-Tracker Green (MTG, a mitochondria-immobilized tracker for mitochondria;[63] Figure S10a,d). Since the quenching effects caused by fluorescence resonance energy transfer (FRET) can be regarded as a proof of colocalization in mitochondria,[64,65] we could deduce that F_{405} was mainly localized in mitochondria. The cells were then treated with 50 μM carbonyl cyanide m-chlorophenylhydrazone (CCCP, an uncoupling reagent of $\Delta\psi_m$[66]) for 2 h, and the fluorescence

https://dx.doi.org/10.1021/acs.analchem.0c01046
Anal. Chem. 2020, 92, 11103−11110

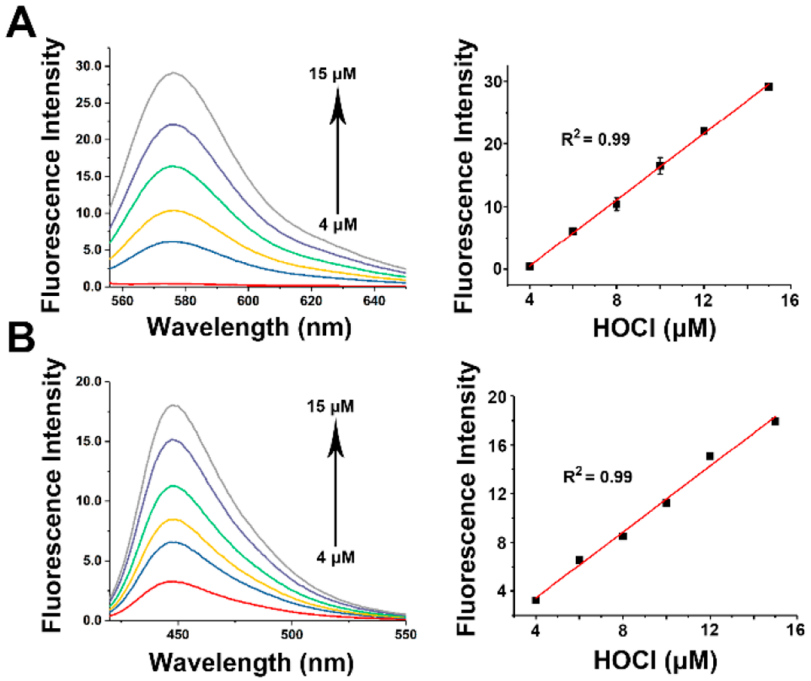

Figure 2. Fluorescent response of 5 μM ZED-1 to 4−15 μM HOCl in PBS buffers (pH 8.0, 50 mM, 0.1% DMSO). (A) Excitation at 543 nm. (B) Excitation at 405 nm.

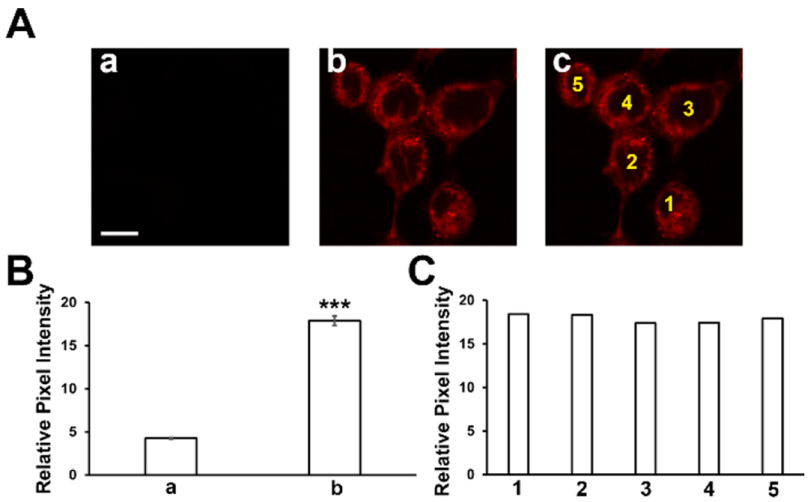

Figure 3. Response of ZED to HOCl in MCF-7 cells. (A) Images of the cells. (a) Cells incubated with 5 μM ZED for 10 min. (b, c) Cells incubated with 5 μM ZED for 10 min and then treated with 40 μM HOCl for 10 min. Images were recorded using excitation wavelength of 543 nm, and band-path emission filter at 553−618 nm. (B) Relative pixel intensity of the related images in (A). The results are presented as mean ± standard deviation (n = 3). The significant difference (***p < 0.001) is performed by Student's t-test. (C) Relative pixel intensity of the cells in (c). Scale bar: 10 μm.

quenching still existed (Figure S10g,j), indicating that F_{405} was retained in mitochondria after mitochondrial depolarization. Meanwhile, F_{405} also had a great overlay with MTG after the same CCCP treatment (Pearson's correlation coefficient was 0.93; Figure S11), which confirmed that F_{405} was retained in mitochondria after mitochondrial depolarization. Within this context, we can see that ZED is mitochondria-immobilized, which is the same as MTG.

We next tested whether the intensity of F_{405} was response to mitochondrial status in living cells. As shown in Figure 1b, F_{405} was faded distinctly when the cells were treated with 50 μM CCCP for 20 s. This fast response indicated that F_{405} real-time responded to $\Delta\psi_m$ in living cells. Since ZED was mitochondria-immobilized and F_{405} changed with pH from 7.4 to 8.0 in cuvettes (Figure S12), this decrease in F_{405} in cells was probably mainly caused by the decrease in mitochondrial pH (normally from 7.4 to 8.0) during loss of $\Delta\psi_m$.[67] When CCCP was removed to regain $\Delta\psi_m$, F_{405} could also recover in cells (Figure S13), confirming that F_{405} real-time detected $\Delta\psi_m$ through pH changes in cells although F_{405} could also be altered by other biological analytes in cuvettes (Figure S14). However, in contrast to the fading (Figure 1b), F_{405} was lightened when the cells were further incubated with CCCP for 2 h to induce opening of the MPT pore (Figure 1c).[68−70] Since many cationic dyes are partly quenched by aggregation in mitochondria,[67] this enhancement in F_{405} was probably caused

https://dx.doi.org/10.1021/acs.analchem.0c01046
Anal. Chem. 2020, 92, 11103−11110

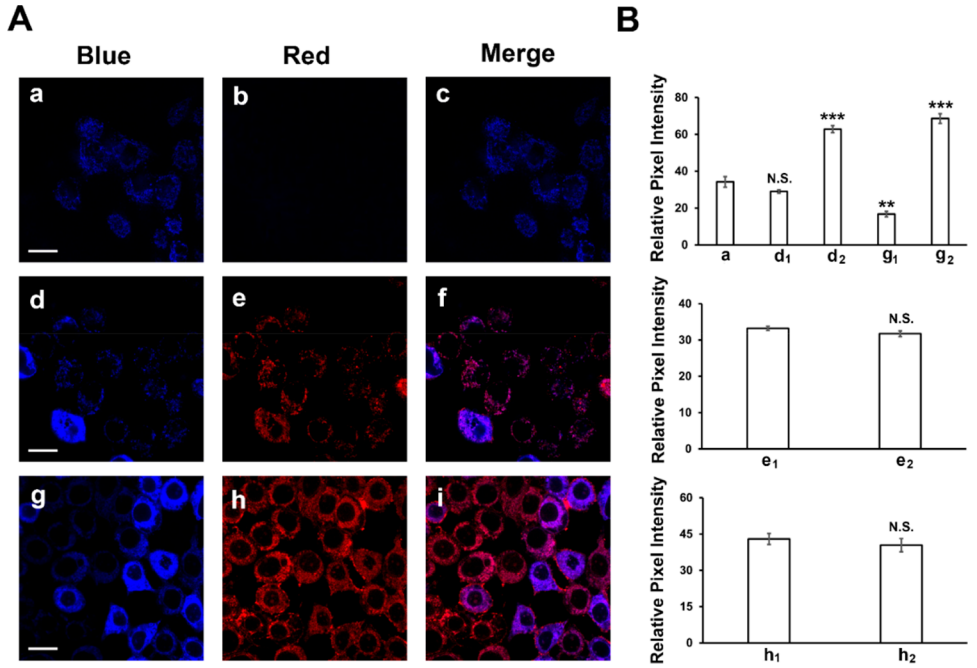

Figure 4. Simultaneous response of ZED to mitochondrial status and HOCl in MCF-7 cells. (A) Images of the cells. (a−c) Cells incubated with 5 μM ZED for 10 min. (d−f) Cells incubated with 5 μM ZED for 10 min and then treated with 80 μM HOCl for 5 min. (g−i) Cells incubated with 5 μM ZED for 10 min and then treated with 80 μM HOCl for 30 min. The cells without lightened F_{405} in (d, e, g, and h) were categorized as d_1, e_1, g_1, and h_1, respectively. The cells with lightened F_{405} in (d, e, g, and h) were categorized as d_2, e_2, g_2, and h_2, respectively. Blue and red channels were recorded using excitation wavelengths of 405 and 543 nm, and band-path emission filters at 417−477 and 553−618 nm, respectively. (B) Relative pixel intensity of the related cells in (A). The results are presented as mean ± standard deviation (n = 3). Significant differences (N.S.: no significant difference; $^{**}p < 0.01$; $^{***}p < 0.001$) are performed by Student's t-test. Scale bar: 20 μm.

by the MPT-mediated swelling of mitochondria in cells.[71] When cyclosporin A (an inhibitor of opening of the MPT pore[72]) was added during the CCCP treatment, this enhancement was also inhibited (Figure S15), indicating F_{405} also detected opening of the MPT pore in cells. In addition, the F_{405} in MCF-7 cells was brighter than that in HBL-100 cells (Figure 1a,d), indicating that F_{405} also differentiated MCF-7 cells from HBL-100 cells. In brief, this study of F_{405} shows that ZED not only differentiates MCF-7 cells from HBL-100 cells but also simultaneously detects $\Delta\psi_m$ and opening of the MPT pore in mitochondria.

After carefully studying F_{405} alone in cells, we then tried to investigate F_{543} in cells. To start with, the response of ZED-1 toward HOCl was tested in cuvettes, given that ZED would immediately transform into ZED-1 in cells. As shown in Figure 2A, F_{543} had a linear relationship with HOCl in 4−15 μM. The red fluorescence was generated within seconds upon the addition of HOCl (Figure S16). However, when the concentration of HOCl was lower than 4 μM, ZED-1 had slightly poor sensitivity to HOCl with a detection limit of 167 nM (Figure S17). A linear relationship with HOCl was also obtained for ZED with a detection limit of 303 nM (Figure S18). Next, we tested whether ZED responded to HOCl in cells. As shown in Figure 3A, F_{543} was turned on brightly after the cells were incubated with 40 μM HOCl. The even distribution of F_{543} in different cells (Figure 3C) showed that the mitochondrial uptakes of ZED in different cells were uniform. Besides, F_{543} also had a good overlay with MTG (Pearson's correlation coefficient was 0.82; Figure S19), indicating that the generated Rhodamine B was retained in mitochondria to a large extent.

Next, the influence of HOCl on F_{405} was investigated in cuvettes. As mentioned before, the rhodamine part of ZED broke away from the skeletal structure to form Rhodamine B once reacting with HOCl. The newly formed Rhodamine B was then separated from 7-hydroxycoumarin, protecting F_{405} from the fluorescence quenching caused by F_{543} in solutions. Very interestingly, as shown in Figure 2B, F_{405} increased instead of decreasing during the generation of F_{543}. A linear relationship with HOCl in 4−15 μM was also achieved for F_{405}. Unlike the distinct fluorescence increase in F_{405}, the absorbance at 405 nm decreased a little after the HOCl treatment (Figure S20), indicating that the concentration of 7-hydroxycoumarin in the ground states did not change much during the fluorescence enhancement. Obviously, the electron-rich rhodamine part had photoinduced electron transfer (PET) to 7-hydroxycoumarin, which mainly influenced the fluorescence intensity in the excited states. This HOCl-induced increase in F_{405} was probably caused by the disappearance of PET after the rhodamine part broke away from ZED-1.

HOCl has been reported to be capable of inducing loss of $\Delta\psi_m$ and opening of the MPT pore in cells,[73,74] so we further tested whether ZED simultaneously detected HOCl and HOCl-induced mitochondrial dysfunction in cells. First of all, we studied whether there was fluorescence quenching between F_{405} and F_{543} in mitochondria. Generally speaking, the Rhodamine B generating F_{543} was separated from the 7-hydroxycoumarin generating F_{405} in mitochondria, so we could employ an extra molecule, Mito-Tracker Red (MTR, a mitochondria-immobilized tracker for mitochondria based on rhodamine dyes[75]), as a substitute for F_{543} to avoid the influence of HOCl on either F_{405} or mitochondrial status in cells. As the incubation went on, MTR emitted similar red

https://dx.doi.org/10.1021/acs.analchem.0c01046
Anal. Chem. 2020, 92, 11103−11110

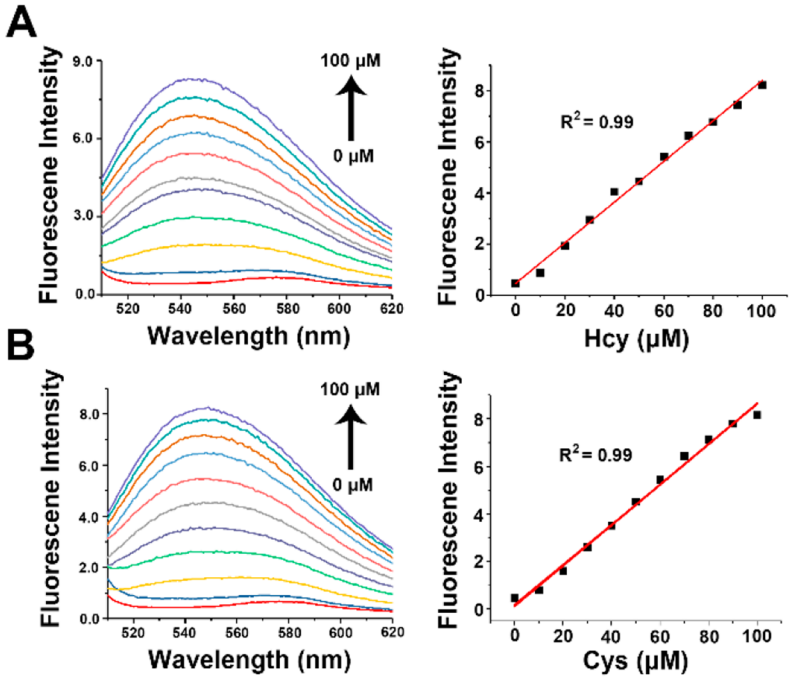

Figure 5. Fluorescent response of 5 μM ZED to 0−100 μM Cys/Hcy in PBS buffers (pH 8.0, 50 mM, 0.1% DMSO), excitation at 488 nm. (A) Hcy and (B) Cys.

fluorescence to F_{543} at about 10 min, while F_{405} was not faded in cells (Figure S21), showing that the fluorescence quenching between F_{405} and F_{543} was very weak in mitochondria. Unlike the fluorescence quenching between F_{405} and MTG in mitochondria, this weak FRET between F_{405} and MTR was probably mainly due to the poor spectral overlap between them. The higher feeding concentration of MTG may also contribute to the fluorescence quenching as FRET only happens within 10 nm and molecules are closer in mitochondria when the concentration is higher.

With this result in hand, we then investigated the influences of HOCl on F_{405} and mitochondrial status in cells. In the presence of 80 μM HOCl for 5 min, F_{405} was lightened in some cells, but was decreased in the others (Figure 4d). When the cells were incubated with HOCl for as long as 30 min, F_{405} was lightened in more cells, but was faded in most of the others (Figure 4g). Considering the weak fluorescence quenching between F_{405} and F_{543} in mitochondria, the faded F_{405} in Figure 4g indicated that loss of $\Delta\psi_m$ was induced by HOCl in cells. Meanwhile, the lightened F_{405} in Figure 4d,g showed that opening of the MPT pore was also induced by HOCl in cells. To the best of our knowledge, this is the first visualized proof in literature that opening of the MPT pore and loss of $\Delta\psi_m$ can be discriminatively induced by HOCl in different cells. Besides, the decreased and faded F_{405} in Figure 4d,g indicated that the HOCl-induced increase in F_{405} was so weak in cells that it could not influence the ability of ZED to sense mitochondrial status. Since ZED accumulated in mitochondria, while the concentration of HOCl decreased a lot in the presence of abundant reductants in cells, it was not strange that little percentage of ZED reacted with HOCl in cells, leading to the weak increase in F_{405}. In contrast to F_{405}, there were not significant differences among the intensities of F_{543} in cells (Figure 4B), indicating that ZED accurately detected HOCl in cells ignoring the impacts of mitochondrial status. This even distribution of F_{543} also showed that the concentration of ZED was not altered much by mitochondrial status in cells, confirming that ZED was mitochondria-immobilized. These results suggest that ZED simultaneously detects HOCl and HOCl-induced mitochondrial dysfunction in cells.

At last, we tested whether ZED simultaneously detected Cys/Hcy, HOCl and mitochondrial status in cells. The response of ZED to Cys/Hcy was first tested in cuvettes and cells. F_{488} was generated gradually in the presence of Cys/Hcy (Figure S22), while a linear relationship in 0−100 μM was observed (Figure 5). The detection limits of Cys and Hcy were 333 nM and 352 nM, respectively. As shown in Figure 6d, F_{405} and F_{488} were turned on with a very poor overlay in cells (Pearson's correlation coefficient was lower than 0.3), indicating that F_{488} was not in mitochondria at all. This distinct localization also showed that F_{488} could not be influenced by mitochondrial status and these two signals were independent from each other in cells. Besides, the fluorescence intensity of F_{488} was much weaker than that of MTG in cells, so F_{488} could not have influenced the experiments involving MTG. When the cells were pretreated with N-ethylmaleimide (NEM, a thiol inhibitor[76]), the green fluorescence was weakened in cells (Figure S23), confirming that F_{488} was generated by the reaction of NBD and Cys/Hcy. After the cells were further treated with HOCl, F_{488} was retained in cells but decreased (Figure 6B). The pictures showed that F_{488} was mainly localized in spots, and became more dispersive during the HOCl treatment, which was probably the reason why F_{488} decreased. However, this retention of F_{488} after HOCl treatment still suggested that ZED simultaneously detected Cys/Hcy and HOCl in cells. In addition, even with the naked eye, we saw that F_{405} was lightened and F_{543} was turned on after the HOCl treatment, indicating that mitochondrial status was altered by HOCl in cells. In this case, together with all the previous experiments, we conclude that ZED simultaneously detects Cys/Hcy, HOCl and mitochondrial status in living cells.

https://dx.doi.org/10.1021/acs.analchem.0c01046
Anal. Chem. 2020, 92, 11103−11110

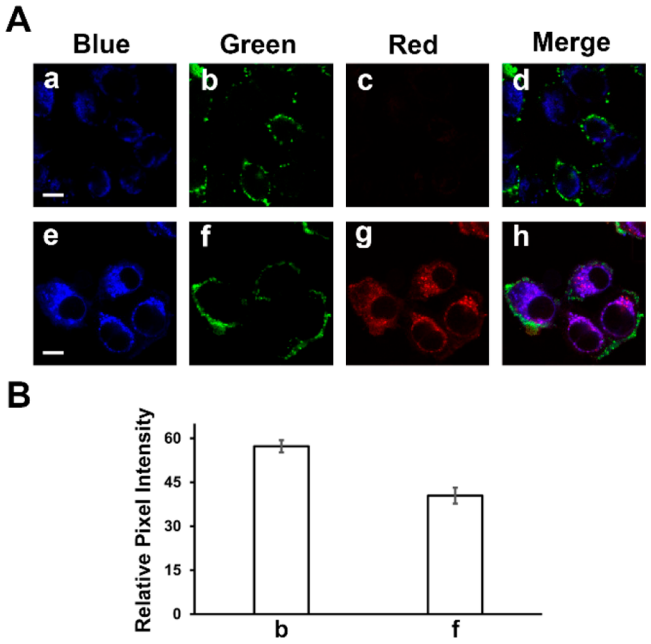

Figure 6. Simultaneous response of ZED to Cys/Hcy, HOCl and mitochondrial status in A549 cells. (A) Images of the cells. (a–d) Cells incubated with 5 μM ZED for 10 min. (e–h) Cells incubated with 5 μM ZED for 10 min and then treated with 80 μM HOCl for 30 min. Blue, green and red channels were recorded using excitation wavelengths of 405, 488, and 543 nm, and band-path emission filters at 417–477, 499–529, and 553–618 nm, respectively. (B) Relative pixel intensity of the related images in (A). The results are presented as mean ± standard deviation (n = 3). Scale bar: 10 μm.

CONCLUSIONS

In summary, we have successfully constructed a unimolecular probe, ZED, which simultaneously detects Cys/Hcy, HOCl, $\Delta\psi_m$, and opening of the MPT pore in cells. Due to the good cell permeability and biocompatibility of ZED, the sensing process is fast, selective, and sensitive in living cancer cells. Moreover, the four outputs have little cross-talk in cells, which is not easy to be achieved even with different probes. ZED is the first probe that simultaneously detects four analytes in cells and the first probe that simultaneously detects $\Delta\psi_m$ and opening of the MPT pore in mitochondria. Besides, ZED also differentiates MCF-7 cells from HBL-100 cells. To construct ZED, we first used imidazolium salt as a multifunctional linker among fluorophores. This simple molecular design provides a feasible strategy to construct multifunctional probes easily. This "four-in-one" approach should stimulate the design and development of new multifunctional probes.

ASSOCIATED CONTENT

Supporting Information

The Supporting Information is available free of charge at https://pubs.acs.org/doi/10.1021/acs.analchem.0c01046.

Experimental materials, general methods, additional figures, synthesis steps, and compounds characterization (PDF)

AUTHOR INFORMATION

Corresponding Authors

Yulei Chang – *State Key Laboratory of Luminescence and Applications, Changchun Institute of Optics, Fine Mechanics and Physics, Chinese Academy of Sciences, Changchun 130033, China;* orcid.org/0000-0001-7223-1797; Email: yuleichang@ciomp.ac.cn

Zhan Shi – *State Key Laboratory of Inorganic Synthesis and Preparative Chemistry, College of Chemistry, Jilin University, Changchun 130012, P. R. China;* orcid.org/0000-0001-9717-1487; Email: zshi@mail.jlu.edu.cn

Authors

Nansong Zhu – *State Key Laboratory of Inorganic Synthesis and Preparative Chemistry, College of Chemistry, Jilin University, Changchun 130012, P. R. China*

Xiaolei Guo – *State Key Laboratory of Inorganic Synthesis and Preparative Chemistry, College of Chemistry, Jilin University, Changchun 130012, P. R. China*

Shirui Pang – *State Key Laboratory of Inorganic Synthesis and Preparative Chemistry, College of Chemistry, Jilin University, Changchun 130012, P. R. China*

Xiaomin Liu – *State Key Laboratory of Integrated Optoelectronics, College of Electronic Science and Engineering, Jilin University, Changchun 130012, China;* orcid.org/0000-0003-4186-9637

Shouhua Feng – *State Key Laboratory of Inorganic Synthesis and Preparative Chemistry, College of Chemistry, Jilin University, Changchun 130012, P. R. China;* orcid.org/0000-0002-6967-0155

Complete contact information is available at: https://pubs.acs.org/10.1021/acs.analchem.0c01046

Notes

The authors declare no competing financial interest.

ACKNOWLEDGMENTS

This work was supported by the National Natural Science Foundation of China (61875191, 21621001, 21771077, and 21771084), the National Key Research and Development Program of China (2016YFB0701100), the 111 projects (B17020), and Jilin Provincial Development and Reform Commission (Grant No: 2018C052-10).

REFERENCES

(1) Bray, F.; Ferlay, J.; Soerjomataram, I.; Siegel, R. L.; Torre, L. A.; Jemal, A. *Ca-Cancer J. Clin.* **2018**, *68* (6), 394–424.

(2) Pierce, M. C.; Javier, D. J.; Richards-Kortum, R. *Int. J. Cancer* **2008**, *123* (9), 1979–1990.

(3) Miao, Y.; Shi, L.; Hu, F.; Min, W. *Phys. Biol.* **2019**, *16* (4), 041003.

(4) Ishizawa, T.; Saiura, A. *Surg. Oncol. Clin. N. Am.* **2019**, *28* (1), 45–60.

(5) Hernot, S.; van Manen, L.; Debie, P.; Mieog, J. S. D.; Vahrmeijer, A. L. *Lancet Oncol.* **2019**, *20* (7), No. e354.

(6) Kobayashi, H.; Longmire, M. R.; Ogawa, M.; Choyke, P. L.; Kawamoto, S. *Lancet Oncol.* **2010**, *11* (6), 589–595.

(7) Heinzmann, K.; Carter, L. M.; Lewis, J. S.; Aboagye, E. O. *Nat. Biomed Eng.* **2017**, *1* (9), 697–713.

(8) Wang, L.; O'Donoghue, M. B.; Tan, W. *Nanomedicine (London, U. K.)* **2006**, *1* (4), 413–26.

(9) Chan, D. C. *Cell* **2006**, *125* (7), 1241–52.

(10) Davis, S.; Weiss, M. J.; Wong, J. R.; Lampidis, T. J.; Chen, L. B. *J. Biol. Chem.* **1985**, *260* (25), 13844–50.

(11) Zorov, D. B.; Juhaszova, M.; Sollott, S. J. *Physiol. Rev.* **2014**, *94* (3), 909–50.

(12) Fulda, S.; Galluzzi, L.; Kroemer, G. *Nat. Rev. Drug Discovery* **2010**, *9* (6), 447–64.

(13) Ly, J. D.; Grubb, D. R.; Lawen, A. *Apoptosis* **2003**, *8* (2), 115−128.
(14) Winterbourn, C. C.; Hampton, M. B.; Livesey, J. H.; Kettle, A. J. *J. Biol. Chem.* **2006**, *281* (52), 39860−9.
(15) Bauer, G. *J. Inorg. Biochem.* **2018**, *179*, 10−23.
(16) Chiang, C. L.; Ledermann, J. A.; Rad, A. N.; Katz, D. R.; Chain, B. M. *Cancer Immunol. Immunother.* **2006**, *55* (11), 1384−95.
(17) Knaapen, A. M.; Gungor, N.; Schins, R. P.; Borm, P. J.; Van Schooten, F. J. *Mutagenesis* **2006**, *21* (4), 225−36.
(18) Geisler, J.; Geisler, S. B.; Lonning, P. E.; Smaaland, R.; Tveit, K. M.; Refsum, H.; Ueland, P. M. *Clinical cancer research: an official journal of the American Association for Cancer Research* **1998**, *4* (9), 2125−8.
(19) Mucciarini, C.; Masoni, F.; Cirilli, C.; Artioli, F.; Cavanna, L.; Conte, P. *Annals of Oncology* **2006**, *17*, 140−140.
(20) Ghanemi, A.; Yoshioka, M.; St-Amand, J. *Cytokine* **2020**, *127*, 154996.
(21) Visscher, M.; Arkin, M. R.; Dansen, T. B. *Curr. Opin. Chem. Biol.* **2016**, *30*, 61−67.
(22) Hasan, T.; Arora, R.; Bansal, A. K.; Bhattacharya, R.; Sharma, G. S.; Singh, L. R. *Exp. Mol. Med.* **2019**, *51* (2), 1.
(23) Martinez, V. G.; Moestrup, S. K.; Holmskov, U.; Mollenhauer, J.; Lozano, F. *Pharmacol. Rev.* **2011**, *63* (4), 967−1000.
(24) Yue, Y.; Huo, F.; Yin, C.; Escobedo, J. O.; Strongin, R. M. *Analyst* **2016**, *141* (6), 1859−73.
(25) Roy, S. S.; Hajnoczky, G. *Methods* **2008**, *46* (3), 213−23.
(26) Zhang, T.; Li, Y.; Zheng, Z.; Ye, R.; Zhang, Y.; Kwok, R. T. K.; Lam, J. W. Y.; Tang, B. Z. *J. Am. Chem. Soc.* **2019**, *141* (14), 5612−5616.
(27) Wu, D.; Chen, L.; Xu, Q.; Chen, X.; Yoon, J. *Acc. Chem. Res.* **2019**, *52* (8), 2158−2168.
(28) Chen, H.; Tang, Y.; Lin, W. *TrAC, Trends Anal. Chem.* **2016**, *76*, 166−181.
(29) Chen, J.; Jiang, X.; Zhang, C.; MacKenzie, K. R.; Stossi, F.; Palzkill, T.; Wang, M. C.; Wang, J. *ACS Sens* **2017**, *2* (9), 1257−1261.
(30) He, H.; Ye, Z.; Xiao, Y.; Yang, W.; Qian, X.; Yang, Y. *Anal. Chem.* **2018**, *90* (3), 2164−2169.
(31) Huang, Z.; Li, N.; Zhang, X.; Wang, C.; Xiao, Y. *Anal. Chem.* **2018**, *90* (23), 13953−13959.
(32) Li, M. Y.; Li, K.; Liu, Y. H.; Zhang, H.; Yu, K. K.; Liu, X.; Yu, X. Q. *Anal. Chem.* **2020**, *92* (4), 3262−3269.
(33) Xie, X.; Tang, F.; Liu, G.; Li, Y.; Su, X.; Jiao, X.; Wang, X.; Tang, B. *Anal. Chem.* **2018**, *90* (19), 11629−11635.
(34) Liu, C.; Li, Z.; Yu, C.; Chen, Y.; Liu, D.; Zhuang, Z.; Jia, P.; Zhu, H.; Zhang, X.; Yu, Y.; Zhu, B.; Sheng, W. *ACS Sens* **2019**, *4* (8), 2156−2163.
(35) Zhang, Z.; Fan, J.; Zhao, Y.; Kang, Y.; Du, J.; Peng, X. *ACS Sens* **2018**, *3* (3), 735−741.
(36) Tang, Y.; Jin, L.; Yin, B. *Anal. Chim. Acta* **2017**, *993*, 87−95.
(37) Petronilli, V.; Miotto, G.; Canton, M.; Brini, M.; Colonna, R.; Bernardi, P.; Di Lisa, F. *Biophys. J.* **1999**, *76* (2), 725−734.
(38) Kim, J. E.; He, Q.; Chen, Y.; Shi, C.; Yu, K. *Biochem. Biophys. Res. Commun.* **2014**, *447* (1), 184−91.
(39) Peruzzo, R.; Szabo, I. *Cancers* **2019**, *11* (6), 761.
(40) Zhang, X.; Xu, L.; Yang, T. *OncoTargets Ther.* **2020**, *13*, 877−888.
(41) Hogan, D. T.; Sutherland, T. C. *J. Phys. Org. Chem.* **2018**, *31* (4), No. e3784.
(42) Begtrup, M. *J. Chem. Soc., Chem. Commun.* **1975**, *9*, 334.
(43) Deponte, M.; Hell, K. *J. Biochem.* **2009**, *146* (5), 599−608.
(44) Komatsu, H.; Miki, T.; Citterio, D.; Kubota, T.; Shindo, Y.; Kitamura, Y.; Oka, K.; Suzuki, K. *J. Am. Chem. Soc.* **2005**, *127* (31), 10798−9.
(45) Sukhanova, A.; Nabiev, I. *Crit. Rev. Oncol. Hematol.* **2008**, *68* (1), 39−59.
(46) Cheng, P.; Miao, Q.; Li, J.; Huang, J.; Xie, C.; Pu, K. *J. Am. Chem. Soc.* **2019**, *141* (27), 10581−10584.
(47) Chen, W.; Pacheco, A.; Takano, Y.; Day, J. J.; Hanaoka, K.; Xian, M. *Angew. Chem., Int. Ed.* **2016**, *55* (34), 9993−6.
(48) Ren, M.; Li, Z.; Deng, B.; Wang, L.; Lin, W. *Anal. Chem.* **2019**, *91* (4), 2932−2938.
(49) Jiao, X.; Xiao, Y.; Li, Y.; Liang, M.; Xie, X.; Wang, X.; Tang, B. *Anal. Chem.* **2018**, *90* (12), 7510−7516.
(50) Cheng, R.; Kong, F.; Tong, L.; Liu, X.; Xu, K.; Tang, B. *Anal. Chem.* **2018**, *90* (13), 8116−8122.
(51) Liu, J.; Liu, M.; Zhang, H.; Wei, X.; Wang, J.; Xian, M.; Guo, W. *Chem. Sci.* **2019**, *10* (43), 10065−10071.
(52) Yang, M.; Fan, J.; Sun, W.; Du, J.; Long, S.; Peng, X. *Dyes Pigm.* **2019**, *168*, 189−196.
(53) Lu, Z.; Lu, Y.; Sun, X.; Fan, C.; Long, Z.; Gao, L. *Bioorg. Chem.* **2019**, *92*, 103215.
(54) Xia, X.; Qian, Y. *Analyst* **2018**, *143* (21), 5218−5224.
(55) Sun, L.; Jiang, Y.; Zhang, C.; Ji, X.; Lv, D.; Xi, Z.; Yi, L. *New J. Chem.* **2018**, *42* (18), 15277−15283.
(56) Qiao, D.; Shen, T.; Zhu, M.; Liang, X.; Zhang, L.; Yin, Z.; Wang, B.; Shang, L. *Chem. Commun.* **2018**, *54* (94), 13252−13255.
(57) Hammers, M. D.; Pluth, M. D. *Anal. Chem.* **2014**, *86* (14), 7135−40.
(58) He, L.; Yang, X.; Xu, K.; Yang, Y.; Lin, W. *Chem. Commun.* **2017**, *53* (98), 13168−13171.
(59) Chen, X.; Wang, X.; Wang, S.; Shi, W.; Wang, K.; Ma, H. *Chem. - Eur. J.* **2008**, *14* (15), 4719−24.
(60) Hou, J.-T.; Li, K.; Yang, J.; Yu, K.-K.; Liao, Y.-X.; Ran, Y.-Z.; Liu, Y.-H.; Zhou, X.-D.; Yu, X.-Q. *Chem. Commun.* **2015**, *51* (31), 6781−6784.
(61) Huang, X.-Q.; Wang, Z.-Y.; Lv, Y.-J.; Shen, S.-L.; Zhu, Y.; Wang, J.; Zhang, Y.-R.; Wang, J.-M.; Ge, Y.-Q.; Cao, X.-Q. *New J. Chem.* **2018**, *42* (14), 11480−11484.
(62) Mummidivarapu, V. V.; Yarramala, D. S.; Kondaveeti, K. K.; Rao, C. P. *J. Org. Chem.* **2014**, *79* (21), 10477−86.
(63) Presley, A. D.; Fuller, K. M.; Arriaga, E. A. *J. Chromatogr. B: Anal. Technol. Biomed. Life Sci.* **2003**, *793* (1), 141−150.
(64) Dykens, J. A.; Fleck, B.; Ghosh, S.; Lewis, M.; Velicelebi, G.; Ward, M. W. *Mitochondrion* **2002**, *1* (5), 461−473.
(65) Feng, R.; Guo, L.; Fang, J.; Jia, Y.; Wang, X.; Wei, Q.; Yu, X. *Anal. Chem.* **2019**, *91* (5), 3704−3709.
(66) Heytler, P. G. *Biochemistry* **1963**, *2* (2), 357−361.
(67) Perry, S. W.; Norman, J. P.; Barbieri, J.; Brown, E. B.; Gelbard, H. A. *BioTechniques* **2011**, *50* (2), 98−115.
(68) Scorrano, L.; Petronilli, V.; Bernardi, P. *J. Biol. Chem.* **1997**, *272* (19), 12295−9.
(69) Lim, M. L. R.; Minamikawa, T.; Nagley, P. *FEBS Lett.* **2001**, *503* (1), 69−74.
(70) Bernardi, P. *J. Biol. Chem.* **1992**, *267* (13), 8834.
(71) Scarlett, J. L.; Murphy, M. P. *FEBS Lett.* **1997**, *418* (3), 282−286.
(72) Minamikawa, T.; Williams, D. A.; Bowser, D. N.; Nagley, P. *Exp. Cell Res.* **1999**, *246* (1), 26−37.
(73) Whiteman, M.; Rose, P.; Siau, J. L.; Cheung, N. S.; Tan, G. S.; Halliwell, B.; Armstrong, J. S. *Free Radical Biol. Med.* **2005**, *38* (12), 1571−84.
(74) Whiteman, M.; Chu, S. H.; Siau, J. L.; Rose, P.; Sabapathy, K.; Schantz, J. T.; Cheung, N. S.; Spencer, J. P.; Armstrong, J. S. *Cell. Signalling* **2007**, *19* (4), 705−14.
(75) Poot, M.; Zhang, Y. Z.; Krämer, J. A.; Wells, K. S.; Jones, L. J.; Hanzel, D. K.; Lugade, A. G.; Singer, V. L.; Haugland, R. P. *J. Histochem. Cytochem.* **1996**, *44* (12), 1363−1372.
(76) Fedotcheva, T. A.; Shimanovskii, N. L.; Kruglov, A. G.; Teplova, V. V.; Fedotcheva, N. I. *Biochemistry (Moscow) Supplement Series A: Membrane and Cell Biology* **2012**, *6* (1), 92−99.

https://dx.doi.org/10.1021/acs.analchem.0c01046
Anal. Chem. 2020, 92, 11103−11110